where
I is the current of the solar PV cell (A)
V is the voltage of the solar PV cell (V)
P is the power of the solar PV cell (W)
I_{sc} is the short-circuit current of the solar PV cell (A)
V_{oc} is the open-circuit voltage of the solar PV cell (V)
I_0 is the reverse saturation current (A)
q is the electron charge (C), q = 1.602 × 10-19 (C)
k is Boltzmann's constant, k = 1.381 × 10-23 (J/K)
T is the absolute temperature (K)

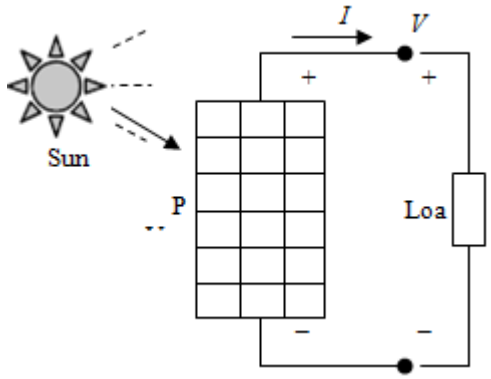

Figure 1: Solar PV panel

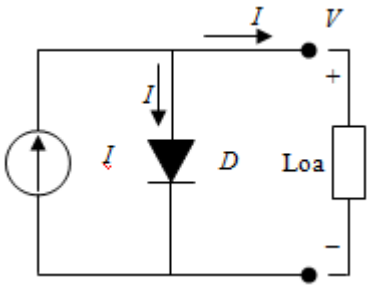

Figure 2: Simple equivalent circuit model of a solar PV cell

It is realized that the solar PV panels are very sensitive to shading. Therefore, a more accurate equivalent circuit for a solar PV cell is presented to consider the impact of shading as well as account for the losses due to the module's internal series resistance, contacts and interconnections between cells and modules, Fig. 3 [1].

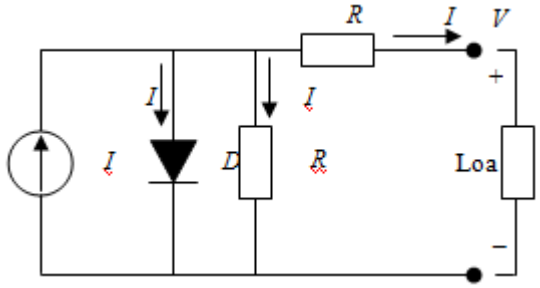

Figure 3: More complex equivalent circuit model of a solar PV cell

Then, the V-I characteristic of a solar PV cell is written as follows:

$$I = I_{sc} - I_0\left(e^{\frac{q(V+IR_s)}{kT}} - 1\right) - \left(\frac{V+IR_s}{R_p}\right) \quad (4)$$

where R_s and R_p are the resistances used to consider the impact of shading and losses. Although, the manufactures try to minimize the effect of both resistances to improve their products, the ideal scenario is not possible.

Two important points of the V-I characteristic that must be pointed out are the open-circuit voltage, V_{oc} and the short-circuit current, I_{sc}. The power generated is zero at both points. The V_{oc} is determined when the output current, I of the cell is zero (I = 0) whereas the I_{sc} is determined when the output voltage, V of the cell is zero (V = 0). The maximum power is generated by the solar PV cell at a point of the current-voltage characteristic where the product (V×I) is maximum. This point is known as the maximum power point (MPP) and is unique. It is obvious that two important factors which have to be taken into account in the electricity generation of a solar PV panel are the irradiation and temperature. These factors strongly affect the characteristics of solar PV panels. As a result, the MPP varies during the day. If the operating point is not close to the MPP, significant power losses occur. Thus, it is essential to track the MPP in all conditions to ensure that the maximum available power is obtained from the solar PV panel.

This problem is entrusted to MPPT algorithms through searching and determining MPPs in various conditions. This paper proposes the improved InC algorithm for tracking MPPs which is presented in more details in the next part.

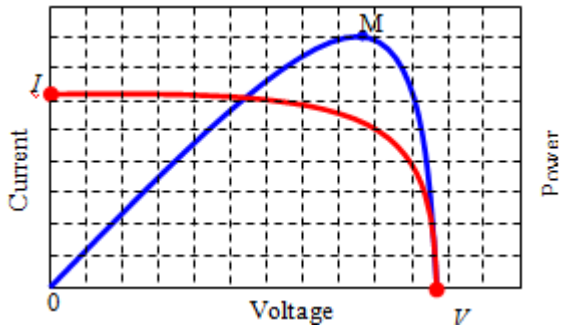

Figure 4: Important points in the V-I and V-P curves of a solar PV panel

3. Improved Incremental Conductance Maximum Power Point Tracking Algorithm

The conventional InC algorithm is reviewed in the part 3.1 of this section followed by a description of the improved InC algorithm.

3.1 Conventional incremental conductance algorithm

The principle of InC algorithm is that the derivative of the power with respect to the voltage or current becomes zero at the MPP, the power increases with the voltage in the left side of the MPP and the power decreases with the voltage in the right side of the MPP [8]-[9].

This description can be re-written in the following simple

equations:

$$\frac{dp}{dv} = 0 \text{ at the left MPP} \quad (5)$$

$$\frac{dp}{dv} > 0 \text{ to the left of the MPP} \quad (6)$$

$$\frac{dp}{dv} < 0 \text{ to the right of the MPP} \quad (7)$$

where

$$\frac{dp}{dv} = \frac{d(iv)}{dv} = I + V\frac{di}{dv} \quad (8)$$

$$\frac{1}{V}\frac{dp}{dv} = \frac{I}{V} + \frac{di}{dv} \quad (9)$$

Therefore, the voltage of the PV panels can be adjusted relative to the MPP voltage by measuring the incremental conductance, *di*/*dv* and the instantaneous conductance, *I*/*V*.

The operation of the InC algorithm is shown in the flow chart, Fig. 5.

It can be realized that the InC algorithm overcomes the oscillation around the MPP when it is reached. When *di*/*dv* = -*I*/*V* is satisfied, which means that the MPP is reached, the operating point is remained. Otherwise, the operating point must be changed, which can be determined using the relationship between *di*/*dv* and -*I*/*V*. Furthermore, the equation (9) shows that:

If $\frac{di}{dv} < -\frac{I}{V}$, then $\frac{dp}{dv} < 0$: the operating point is to the right of the MPP.

If $\frac{di}{dv} > -\frac{I}{V}$, then $\frac{dp}{dv} > 0$: the operating point is to the left of the MPP.

Additionally, the InC algorithm can track the MPP in the case of rapidly changing atmospheric conditions easily, because this algorithm uses the differential of the operating point, *dp*/*dv*. Basically, the algorithm can move the operating point towards the MPP under varying atmospheric conditions.

Nevertheless, the InC algorithm has the disadvantage which requires the control circuit with a higher system cost. It is also required a fast computation for the incremental conductance. If the speed of computation is not satisfied under varying atmospheric conditions, the operating point towards the MPP cannot be guaranteed.

3.2 Improved incremental conductance algorithm

In order to overcome the disadvantages of the conventional InC algorithm, an improved InC algorithm is proposed. The proposed InC algorithm can reduce the main drawbacks commonly related to the InC algorithm.

Firstly, the computation for the differential of the operating point, dp/dv is simplified by the following approximation:

$$\frac{dp}{dv} = \frac{P(k) - P(k-1)}{V(k) - V(k-1)} \quad (10)$$

Secondly, the InC algorithm is combined with the Constant Voltage (CV) algorithm [10]-[11] for the estimation of the MPP voltage which can limit the search space for the InC algorithm.

Basically, the CV algorithm applies the operating voltage at the MPP which is linearly proportional to the open circuit voltage of PV panels with varying atmospheric conditions. The ratio of V_{MPP}/V_{oc} is commonly used around 76% [18].

Thus, the improved InC algorithm is implemented to divide the P-V characteristic into three areas such as area 1, area 2 and area 3, where the area 1 is from 0 to 70%V_{oc}, the area 2 is from 70%V_{oc} to 80%V_{oc} and the area 3 is from 80%V_{oc} to V_{oc}. The area 2 is the area including the MPP, Fig. 6.

It can be realized that the improved InC algorithm only needs to search the MPP within the area 2, from 70%V_{oc} to 80%V_{oc}. This means that:

$$V_{ref} = (70\% - 80\%)V_{oc} = (V_1 - V_2) \quad (11)$$

In the improved InC algorithm, the MPPT system momentarily sets the PV panels current to zero and allow measuring the panels' open circuit voltage. The operation of the improved InC algorithm is shown in the flow chart, Fig. 7.

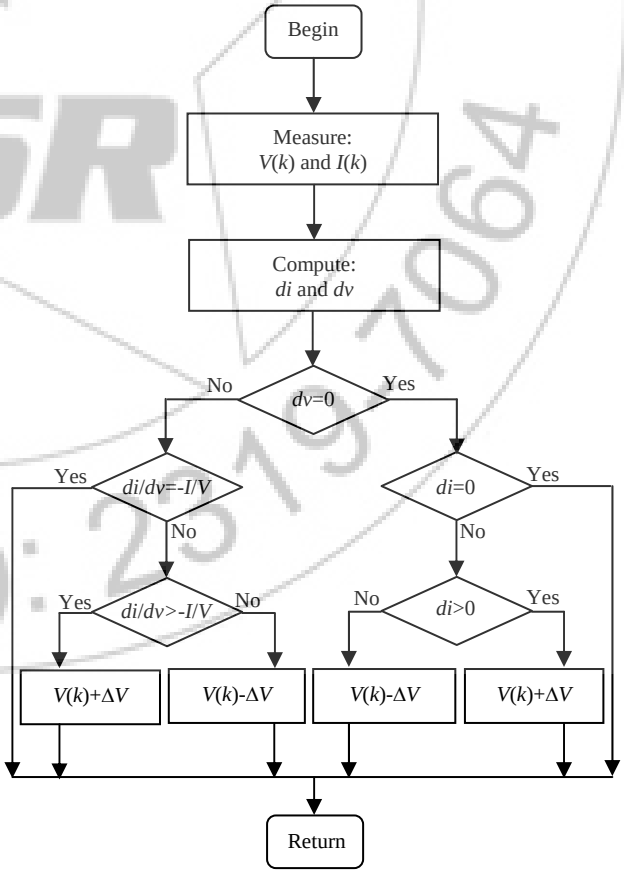

Figure 5: Flow chart of the InC algorithm

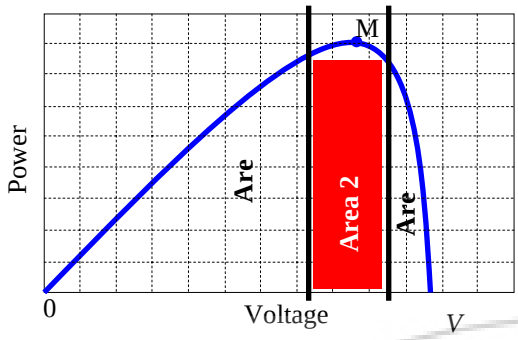

Figure 6: Area partition of the P-V characteristic

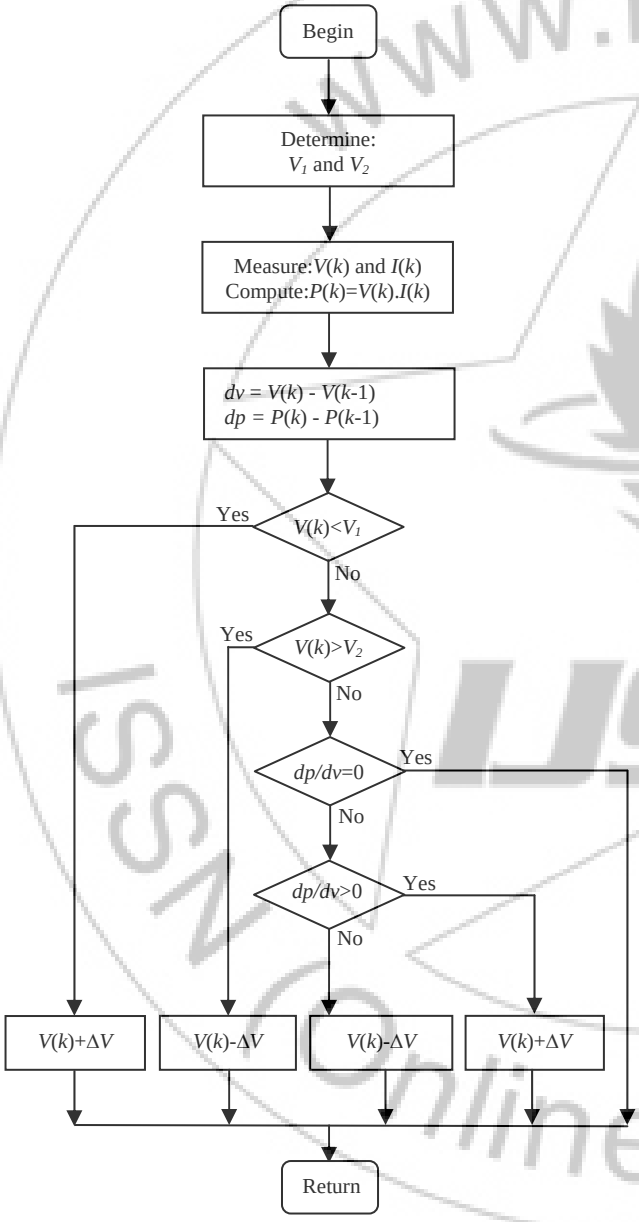

Figure 7: Flow chart of the improved InC algorithm

4. Simulation Results

Simulations are performed using MATLAB/SIMULINK software for tracking MPPs of the solar PV panel whose specifications and parameters are listed in Table 1. The solar PV panel provides a maximum output power at a MPP with V_{MPP} and I_{MPP}. The MPP is defined at standard test condition (STC) of the irradiation, 1 kW/m2 and module temperature, 25 ^{0}C but this condition does not exist most of the time. The following simulations are implemented to confirm the effectiveness of the proposed algorithm which is compared that of the other algorithms such as the P&O and InC algorithms with two combined panels.

Case 1: It is assumed that the module temperature is constant, T^0C = 25 ^{0}C in the simulation. Fig. 8 describes the variation of the solar irradiation where 0 s ≤ t < 1 s: G = 0.25 kW/m^2; 1 s ≤ t < 2 s: G = 0.5 kW/m^2; 2 s ≤ t < 3 s: G = 0.75 kW/m^2; 3 s ≤ t < 4 s: G = 1 kW/m^2 and 4 s ≤ t ≤ 5 s: G = 0.25 kW/m^2. Then, the obtained output powers are shown as in Fig. 9 with the P&O algorithm, in Fig. 10 with the InC algorithm and in Fig. 11 with the improved InC algorithm under the variation of the solar irradiation.

Case 2: It is assumed that the module temperature is changed in the simulation where 0 s ≤ t < 1 s: T^0C = 25 ^{0}C; 1 s ≤ t < 2 s: T^0C = 30 ^{0}C; 2 s ≤ t < 3 s: T^0C = 35 ^{0}C; 3 s ≤ t < 4 s: T^0C = 40 ^{0}C; 4 s ≤ t ≤ 5 s: T^0C = 25 ^{0}C, Fig. 12. The variation of the solar irradiation is described in the Fig. 8. Then, the obtained output powers are shown as in Fig. 13 with the P&O algorithm, in Fig. 14 with the InC algorithm and in Fig. 15 with the improved InC algorithm under the variation of the solar irradiation.

It can be realized that the simulation results of the cases with the improved InC algorithm are always better than the cases with the P&O and InC algorithms, Figs. 9-11 and Figs. 13-15 which are shown through the algorithm convergence and the MPPs' tracking ability, especially with the rapid variation of the temperature solar irradiation, case 2, Fig. 8 and Fig. 12. This means that the drawbacks of the conventional InC algorithm have been overcome using the proposed InC algorithm.

5. Conclusions

In this paper, an improvement of the conventional InC algorithm has been proposed for tracking MPPs of a solar PV panel, known as an improved InC algorithm. This algorithm improves the conventional InC algorithm with the approximation which reduces the computation burden as well as the application of the CV algorithm which increases the convergence speed. This improvement overcame the existing drawbacks of the conventional InC algorithm. The simulation results confirm the validity of the proposed algorithm. The tracking ability of the MPP and obtained output power by the improved InC algorithm are always better than those using the P&O and conventional InC algorithms, especially under the rapid variation condition of the temperature and solar irradiation.

6. Future works

In this parameter identification application, it is assumed that no measurement noise is available and the solar PV panels are always operated under ideal conditions such as no shading conditions, same panels with the same characteristic. Thus, it would be useful to examine the effects in future

research.

Experimental results for the MPPT strategy of the solar PV panels would give a valuable confirmation of the simulation results obtained.

Reference

[1] G. M. Master, Renewable and efficient electric power systems, A John Wiley & Sons, Inc., Publication, 2004.
[2] R. Faranda and S. Leva, "Energy comparison of MPPT techniques for PV systems," WSEAS Trans. Power Syst., vol.3, iss.6, pp. 446-455, 2008.
[3] R. Sridhar, S. Jeevananthan, N. T. Selvan and P. V. Sujith Chowdary, "Performance improvement of a photovoltaic array using MPPT P&O technique," IEEE Int. Conf. Commun. Control and Comput. Technol., pp. 191-195, 2010.
[4] N. M. Razali and N. A. Rahim, "DSP-based maximum peak power tracker using P&O algorithm," IEEE First Conf. Clean Energy and Technol., pp. 34-39, 2011.
[5] L. Chun-Xia, L. Li-qun, "An improved perturbation and observation MPPT method of photovoltaic generate system," 4th IEEE Conf. Ind. Electron. and Appl., ICIEA 2009, pp. 2966-2970, 2009
[6] Y. Jung, J. So, G. Yu and J. Choi, "Improved perturbation and observation method (IP&O) of MPPT control for photovoltaic power systems," 31st IEEE Photov. Specialists Conf., pp. 1788-1791, 2005.
[7] X. Liu, L. A. C. Lopes, "An improved perturbation and observation maximum power point tracking algorithm for PV arrays," IEEE 35th Annual Power Electron. Specialists Conf., pp. 2005-2010, 2004.
[8] B. Liu, S. Duan, F. Liu and P. Xu, "Analysis and improvement of maximum power point tracking algorithm based on incremental conductance method for photovoltaic array," 7th Int. Conf. Power Electron. and Drive Syst., PEDS 2007, pp. 637-641, 2007.
[9] W. Ping, D. Hui, D. Changyu and Q. Shengbiao, "An improved MPPT algorithm based on traditional incremental conductance method," 4th Int. Conf. Power Electron. Syst. and Appl, PESA 2011, pp. 1-4, 2011.
[10] Y. Zhihao and W. Xiaobo, "Compensation loop design of a photovoltaic system based on constant voltage MPPT," Asia-Pacific Power and Energy Eng. Conf., APPEEC 2009, pp. 1-4, 2009.
[11] K. A. Aganah and A. W. Leedy, "A constant voltage maximum power point tracking method for solar powered systems," IEEE 43rd Southeastern Sym. Syst. Theory, SSST 2011, pp. 125-130, 2011.
[12] P. Q. Dzung, L. D. Khoa, H. H. Lee, L. M. Phuong and N. T. D. Vu, "The new MPPT algorithm using ANN based PV," Int. Forum on Strategic Technology, IFOST 2010, pp. 402-407, 2010.
[13] R. Ramaprabha, V. Gothandaraman, K. Kanimozhi, R. Divya and B. L. Mathur, "Maximum power point tracking using GA-optimized artificial neural network for solar PV system," 1st Int. Conf. Electr. Energy Syst., ICEES 2011, pp. 264-268, 2011.
[14] S. J. Kang, J. S. Ko, J. S. Choi, M. G. Jang, J. H. Mun, J. G. Lee and D. H. Chung, "A novel MPPT control of photovoltaic system using FLC algorithm," 11th Int. Conf. Contr., Autom. and Syst., pp. 434-439. 2011.
[15] V. Padmanabhan, V. Beena and M. Jayaraju, "Fuzzy logic based maximum power point tracker for a photovoltaic system," Int. Conf. Power, Signals, Contr. and Comput., EPSCICON 2012, pp. 1-6, 2012.
[16] Md. A. Azam, S. A. A. Nahid, M. M. Alam and B. A. Plabon, "Microcontroller based high precision PSO algorithm for maximum solar power tracking," Conf. Inf., Electron. and Vision, pp. 292-297, 2012.
[17] K. Ishaque, Z. Salam, M. Amjad and S. Mekhilef, "An improved particle swarm optimization (PSO)-based MPPT for PV with reduced steady-state oscillation," IEEE Trans. Power Electron., pp. 3627-3638, 2012.
[18] J. H. R. Enslin, M. S. Wolf, D. B. Snyman and W. Sweigers, "Integrated photovoltaic maximum power point tracking converter," IEEE Trans. Ind. Elec., vol. 44, no. 6, pp. 769-773, 1997.

Table 1: Specifications and parameters of the solar PV panel

Maximum power, P_{max}	80 W
Voltage at P_{max}, V_{MPP}	17.96 V
Current at P_{max}, I_{MPP}	4.60 A
Short-circuit current, I_{sc}	4.92 A
Open-circuit voltage, V_{oc}	21.74 V
Panel series resistance, R_s	0.36 Ω
Panel parallel (shunt) resistance, R_p	1217 Ω

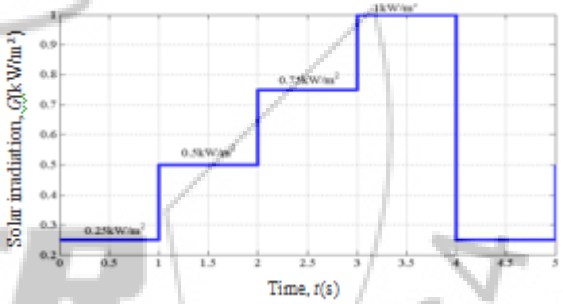

Figure 8: Description of the variation of the solar irradiation

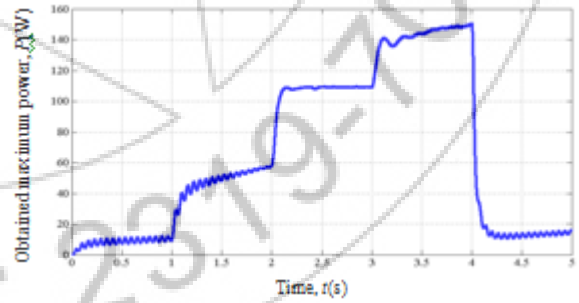

Figure 9: Obtained maximum output power with the P&O algorithm under the variation of the solar irradiation

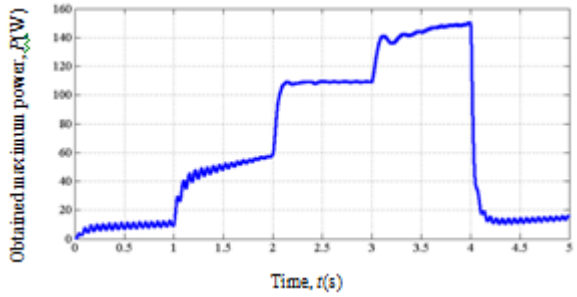

Figure 10: Obtained maximum output power with the InC algorithm under the variation of the solar irradiation

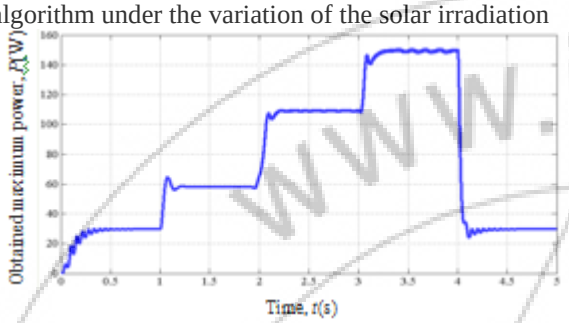

Figure 11: Obtained maximum output power with the improved InC algorithm under the variation of the solar irradiation

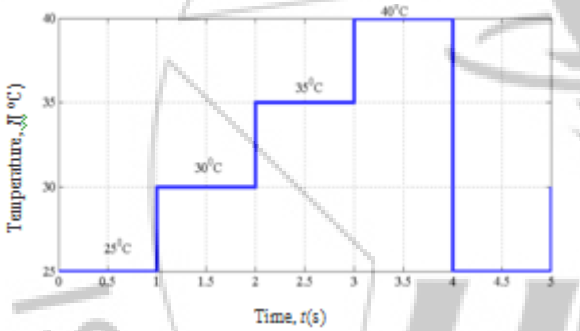

Figure 12: Description of the temperature variation

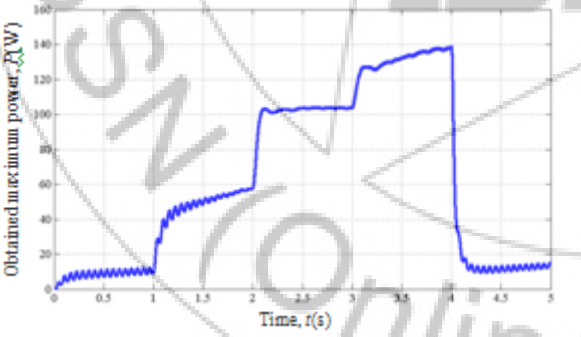

Figure 13: Obtained maximum output power with the P&O algorithm under the variation of the temperature and solar irradiation

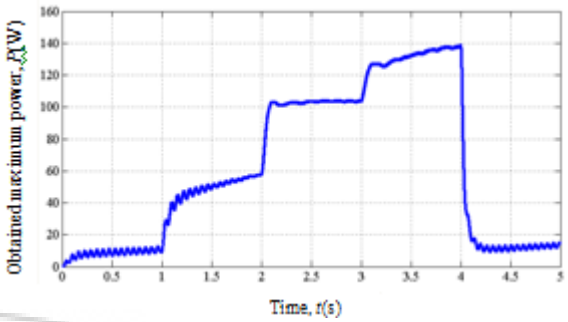

Figure 14: Obtained maximum output power with the InC algorithm under the variation of the temperature and solar irradiation

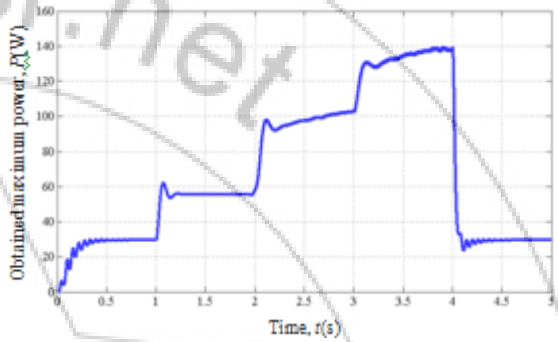

Figure 15: Obtained maximum output power with the improved InC algorithm under the variation of the temperature and solar irradiation

Author Profile

Duy C. Huynh received the B.Sc. and M.Sc. degrees in electrical and electronic engineering from Ho Chi Minh City University of Technology, Ho Chi Minh City, Vietnam, in 2001 and 2005, respectively and Ph.D. degree from Heriot-Watt University, Edinburgh, U.K., in 2010. In 2001, he became a Lecturer at Ho Chi Minh City University of Technology. His research interests include the areas of energy efficient control and parameter estimation methods of induction machines and renewable sources.